

THE EFFECT OF LEAD ON THE HOT WORKABILITY OF AUSTENITIC STAINLESS STEEL WITH A SOLIDIFICATION STRUCTURE

Received – Prispjelo: 2008-10-12
Accepted – Prihvaćeno: 2008-12-20
Preliminary paper – Prethodno priopćenje

The impurities sulphur, phosphorus, lead, bismuth, tin and antimony affect the hot workability of stainless steels. In this study we show that lead segregate to phase and solidification-grain boundaries, where cracks appear during hot deformation. The workability was tested by the hot bending of laboratory steels.

Key words: austenitic stainless steel, hot workability, impurities, lead

Utjecaj olova na toplo preoblikovanje austenitnog nehrđajućeg čelika s ljevanom strukturom.

Nečistoće poput sumpora, fosfora, olova, bizmuta i antimona negativno utječu na toplo preoblikovanje nehrđajućih čelika. U ovaj je studiji pokazano, da olovo segregira na granicama zrna skrućivanja gdje se mogu pojaviti pukotine za vrijeme tople deformacije. Toplo preoblikovanje laboratorijski dobivenih čelika ispitano je metodom toplog savijanja.

Gljučne riječi: austenitni nehrđajući čelik, toplo preoblikovanje, nečistoće, olovo

INTRODUCTION

The impurities sulphur, phosphorus and oxygen, etc. are introduced into steels with the charge, metallic and non-metallic additions during melting and during the secondary treatment of the molten steel. With the increasing use of steel scrap, the content of some impurities has increased. Their removal requires additional processing, or, as in the case for lead, it cannot be achieved. It is less expensive to remove the sulphur, since a content of 0,001 % can be achieved by industrial processing, while, for example, reducing the content of lead, phosphorus, tin and antimony requires a clean charge and additives are more suitable. Some elements, e.g., copper and tin, are not oxidised during the soaking of the steel and are enriched in the metal at the surface and at the grain boundaries, emerging on the surface and inducing hot shortness in structural steels [1].

This kind of brittleness is not meant for stainless steels, because the solubility of copper and tin is increased in austenite with a sufficient content of nickel [2].

The melt-processing temperature is sufficient for the partial volatilization of lead and bismuth, especially during the secondary vacuum treatment, since at high processing temperatures both elements have a high vapour pressure [3]. The non-evaporated lead is found mostly as a liquid residue on the bottom of the furnace and, as shown later, it is found in the solid steel as very

small spherical inclusions accumulated at the solidification boundaries. These inclusions, which in reality are droplets of liquid lead, form when the limit of the lead's solubility in liquid steel is exceeded. This formation must take place below the monotectic temperature.

The effect of lead on the hot workability of stainless steels

All the impurities that segregate at the grain and solidification boundaries decrease the hot workability to a different extent for different elements, since, according to ref. [4], the enrichment of an element at a grain boundary is inversely proportional to its solid solubility in the matrix. For the effect of the most harmful elements, termed as $w.(Pb_{eq.})$, the following empirical relation was proposed [5-7].

$$(Pb_{eq.}) = (Pb) + 4(Bi) + 0,025(Sb) + 0,01(Sn) + 0,007(As) \quad (1)$$

with the content of the element in wt %.

The effect of impurities on the workability is much stronger in the case of solidification to austenite and the hot elongation decreases strongly with an increased value for $Pb_{eq.}$ [6]. It was found that with hot tensile tests the elongation is sufficient with $Pb_{eq.}$ lower than 0,005 % for steels with a solidification to δ -ferrite, while for steels with a solidification to austenite the value of $Pb_{eq.}$ should be lower than 0,003 % [6].

According to the iron side of the binary equilibrium diagram Fe-Pb [8], the solid solubility of lead in the molten steel is limited. It is reported [8] according to

F. Tehovnik, F. Vodopivec, B. Arzenšek, R. Celin, Institute of Metals and Technology, Ljubljana, Slovenia

Araki [9] and Kubaschewsky [10] that the solubility of lead is 0,054 % Pb in the temperature range 1650 °C to 1600 °C. The solid solubility at the monotectic temperature (~ 1530 °C) is, according to the same authors, of $2,7 \times 10^{-4}$ % Pb. Two equations describing the solubility of lead in molten iron have been reported [10, 11].

$$\lg(w.\%Pb) = -11100/T + 5,57 \quad (2)$$

with the content of the element in wt %.

$$\lg(x.\%Pb) = -13400/T + 6,16 \quad (3)$$

with the content of the element in atomic %.

Experience shows that lead, with a greater density than iron and a high vapour pressure [3], is partially volatilised from the melt, partially deposited on the bottom of the furnace and, as in lead-free machining steels [12] partially found in small droplets in the solidified steel.

Depending on the content of the main alloying elements and impurities the solidification of austenitic stainless steels can proceed according to two mechanisms [13, 14].

- melt \rightarrow austenite with increased content of nickel \rightarrow δ -ferrite from the residual interdendritic melt enriched in chromium, or
- melt \rightarrow δ -ferrite enriched in chromium \rightarrow austenite with solidification of the residual interdendritic melt and/or a solid transformation δ -ferrite \rightarrow austenite during cooling.

Some elements, e.g., molybdenum, silicon and titanium, enhance the solidification via δ -ferrite, others, e.g., carbon, manganese and copper, enhance the solidification via austenite.

EXAMINATION

All the tests were carried out with specimens that have a solidification structure. The specimens for the hot-bending tests were prepared by casting laboratory steel in a heated grey-iron mould of section 20×40 mm. The chemical composition of the investigated steel is shown in Table 1. The content of lead in the 316L(Pb) steel was approximately 2,5 times higher than that reported for the inducing of hot shortness [15], and according to our industrial experience, five times higher than that critical for the appearance of edge cracks during the hot rolling of 200 mm continuously cast slabs.

The aim of the bending tests was to establish the effect of lead on the formation of cracks during hot-stretching deformation. The specimens were heated to temperatures of 1050 °C, 1150 °C and 1250 °C, held for 5 min or 40 min, bent by 90° on a round mandrel and quenched in water. The time from the taking out of the furnace to the end of the bending was only a few seconds. It is assumed, therefore, that the deformation temperature was equal to the heating temperature. The cracks were found by visual inspection and confirmed with liquid penetrant tests. The hot crack surface was then opened by bending the cut-out specimens cooled in

liquid nitrogen and investigated with scanning electron microscopy (SEM) and EDS analysis.

The maximum stretching tensile deformation was found for bend specimens of 29 %. The initial shape of the cross-section of the specimen preserved after the bending confirms that the deformation at the surface of the specimen was almost exclusively uniaxial stretching.

Table 1. Chemical composition of the investigated steel AISI 316L(Pb)

Elements/wt. %									
C	Si	Mn	P	S	Cr	Ni	Cu	Mo	Pb
0,03	0,6	1,43	0,026	0,001	16,57	10,36	0,37	2,14	0,0083

EXAMINATION RESULTS

Hot-bending tests

During a visual examination of the tensile surface of the hot-bend specimens of the leaded AISI 316L(Pb) steel fine transverse cracks were found, more frequently near the specimens' borders. This was confirmed with liquid penetrant tests (Figure 1). A microscopic examination of the cracked section showed the cracks to be intergranular and to have a surface covered with a thin layer of oxide. In the metal near the crack lip, small spherical inclusions (Figure 2) were found and confirmed to be pure lead (Figure 3, Table 2). No lead inclusions were found at a greater distance from the boundary. The solubility of the lead is greater for the liquid than for the solid steel and, with the advance of the solidification front, the content of lead in the remnant liquid was increased. The end product of the solidification is a nanotectic consisting of solid steel with a very low content of lead in solid solution and droplets of lead that solidify at a much lower temperature. The results of the EDS analysis of the lead inclusions in Table 2 are approximate, because the size of the inclusions was smaller than the depth and the lateral penetration of the electron beam, which meant that elements from the matrix were detected. The analysis showed a high lead content in the inclusions and, considering that iron, nickel and chromium are virtually insoluble in lead, the conclusion that the inclusions are virtually pure lead is justified.

Thin platelets were cut out from the cracked area of the bend surface, cooled in liquid nitrogen, fractured by bending around a thin mandrel and the opened, cracked surface was examined with SEM. The macrophotography fracture surface of the specimen is shown in Figure 4.

In Figure 5 part of the cracked surface is shown, where two mechanisms of crack propagation are visible: the area of dimpled ductile fracturing of the cooled steel and the area of propagation during the solidification of the grain boundaries (Figure 6). This area of the surface in Figure 5 was covered with a thin layer of oxide, oblit-

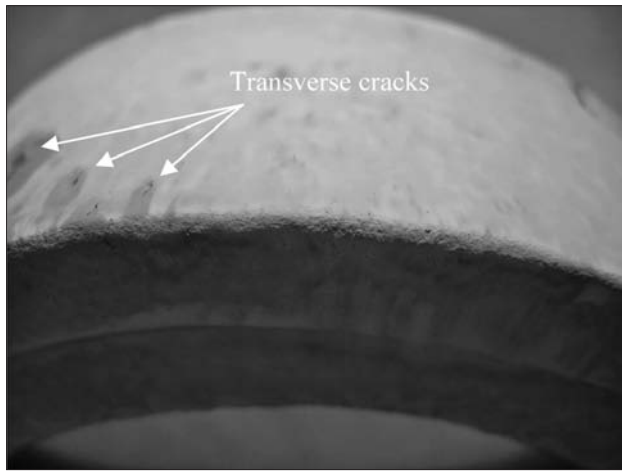


Figure 1. Hot bending specimen, view from convex sides (penetrant test)

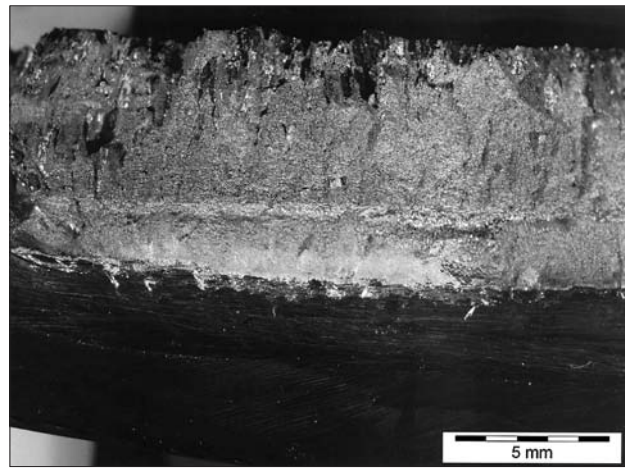


Figure 4. Macrophotography fracture surface of the specimen broken after cooling in liquid nitrogen

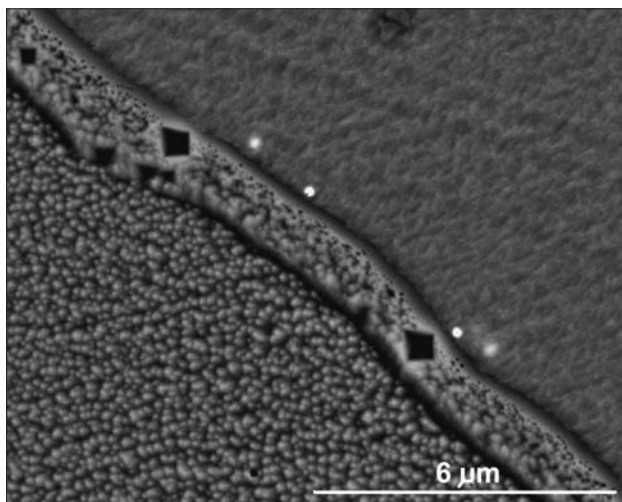


Figure 2. SEM micrograph of the grain-boundary region with lead inclusions

Table 2. Results of the EDS analysis at points marked in Figure 3

Element/wt.%	Si	Cr	Mn	Fe	Ni	Mo	Pb
Spectrum 1	0,40	15,82	1,65	61,66	9,30	2,02	9,15
Spectrum 2	0,40	13,78	1,47	50,83	7,82		25,69
Spectrum 3	0,54	14,23	0,89	51,14	7,28		25,92
Spectrum 4	0,65	16,96	1,46	67,27	10,89	2,77	
Spectrum 5	0,62	16,45	1,60	68,36	10,90	2,07	
Spectrum 6	0,60	16,72	1,42	67,97	10,72	2,57	

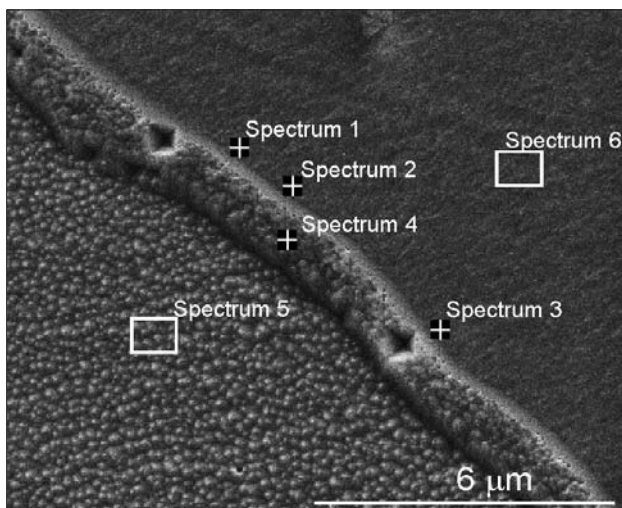


Figure 3. Points of EDS analysis in Figure 2

lished by point analysis, confirm the presence of lead inclusions on the hot-fracture surface and the presence of liquid droplets of lead at the solidification grain boundaries during hot bending. No other impurities were found in the interdendritic surface in Figure 6. We can conclude that grain-boundary fracturing was induced by the presence of droplets of lead and that lead droplets did drop out mostly from the cracked surface when it was opened because the size of the solid lead inclusion was smaller than the corresponding microscopic hollow formed around the liquid droplet during the steel's solidification.

erating the fracture micromorphology and confirming that the surface was formed by cracking during the hot bending. Only rare and small lead inclusions were found on the interdendritic, cracked surface (Figure 7). Their size did not allow a reliable chemical analysis; however, the line scanning and the content of 4,4 % Pb, estab-

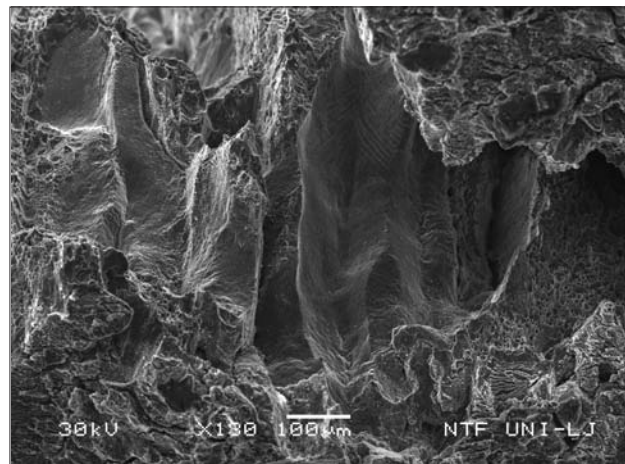


Figure 5. Fracture surface of the specimen broken after cooling in liquid nitrogen

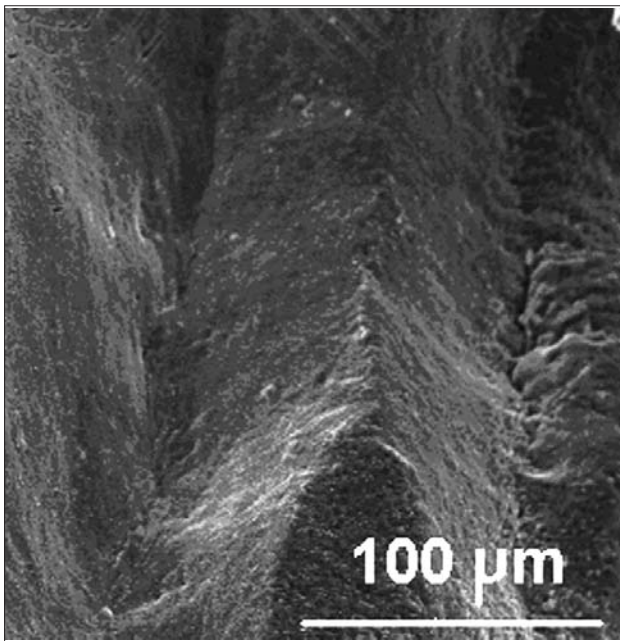


Figure 6. Detail of the intergranular surface in Figure 5

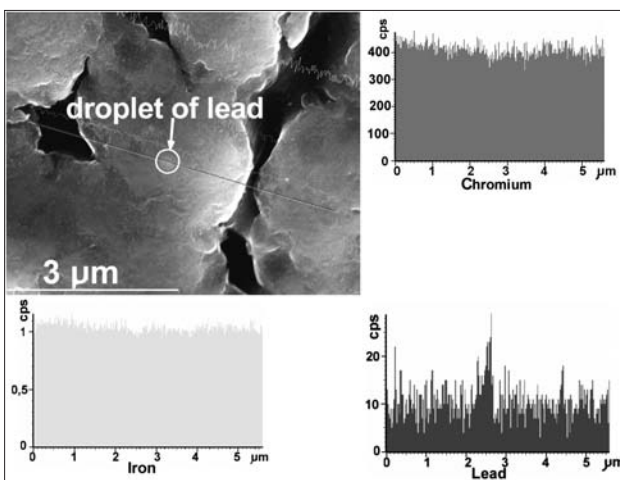


Figure 7. Image and line scanning on the interdendritic, cracked surface with droplets of lead

CONCLUSION

Hot-bending tests were performed on one laboratory austenitic stainless steel with up to 0,0083 % Pb. The test were performed in the temperature range from 1050 °C to 1250 °C. The maximum deformation was 29 % during hot bending. The deformed specimens were investigated with optical and SE microscopy and EDS analysis. Transverse cracks were found on the surface of some specimens deformed with the hot bending.

The solubility of lead is greater in liquid than in solid steel. During solidification the lead is rejected from the

melt, and small droplets are formed and accumulated on boundaries of solidification grains at the monotectic temperature. During metallographic examinations, hot cracks and lead inclusions were observed at some of the solidification boundaries. On the surface of the opened cracks a thin layer of oxide was found, the presence of lead inclusions were confirmed, and the cracking at the deformation temperature was also confirmed.

The following experimental findings of this investigations are of significance for the understanding of the hot workability of stainless steels containing of lead with the as-solidified microstructure consisting of austenite and of δ -ferrite:

- droplets of lead are enriched at the solidification boundaries;
- interphase segregation and the accumulation of lead inclusions decrease the steel's hot workability.

REFERENCES

- [1] F. Vodopivec, M. Torkar, M. Debelak, M. Kmetič, F. Haler, F. Kaučič, *Mater. Sci. Technol.*, (1988) 4, 917
- [2] G. L. Fisher: *J. Iron Steel Inst.*, (1969) 207, 1010
- [3] J. F. Elliott, M. Gleiser: *Thermochemistry for steelmaking*, Vol.I, 270; (1960), Reading, Addison-Wesley publishing Company
- [4] C. L. Briant, *Mater. Sci. Technol.*, (2001) 17, 1317-1323.
- [5] W. Runsheng, *Special steel*, (2000) 21, 10-13.
- [6] L. Myllykoski, N. Suutala, *Metals Technology*, (1983) 10, 453-460.
- [7] L. Ľ. Norström, *Scandinavian J. of Metallurgy*, (1979) 8, 95-96.
- [8] B. Burton, *J. of Phase Equil.*, (1991) 12, 200-202.
- [9] T. Araki, *Trans. Nat. Res. Inst. Met. Tokyo*, (1991) 5.
- [10] O. Kubaschewski, *Iron-Binary Phase Diagrams*, New York, Springer-Verlag (1982), 87-88.
- [11] A. N. Morozov, Yu. A. Ageyev: *Russ. Metall.*, (Equi Diagram; Experimental), (1971) 4, 435.
- [12] A. Razinger: *Železarski zbornik*, (1974) 8, 99-109.
- [13] R. Honeycombe, P. Hancock, *Steels Microstructure and Properties*, 2nd ed; 1995, Cambridge, University of Cambridge
- [14] J. R. Davis et al.: *ASM Specialty Handbook: Stainless Steels*; 1996, Ohio, ASM International
- [15] L. G. Ljugström, *Scandinavian J. of Metallurgy*, (1977) 6, 176-184.

Note: The responsible translator for English language is Franc Vodopivec, IMT - Ljubljana.